JOURNAL OF GEOPHYSICAL RESEARCH: SOLID EARTH, VOL. 118, 165–182, doi:10.1029/2012JB009486, 2013

Do earthquakes talk to each other? Triggering and interaction of repeating sequences at Parkfield

Kate Huihusan Chen,[1] Roland Bürgmann,[2,3] and Robert M. Nadeau[3]

Received 29 May 2012; revised 7 November 2012; accepted 8 November 2012; published 29 January 2013.

[1] Knowledge of what governs the timing of earthquakes is essential to understanding the nature of the earthquake cycle and to determining earthquake hazard, yet the variability and controls of earthquake recurrences are not well established. The large population of small, characteristically repeating earthquakes at Parkfield provides a unique opportunity to study how the interaction of earthquakes affects their recurrence properties. We analyze 112 M −0.4~3.0 repeating earthquake sequences (RESs) to examine the triggering effect from nearby microseismicity. We find that the repeating events with a smaller number of neighboring earthquakes in their immediate vicinity tend to recur in a more periodic manner (i.e., the coefficient of variation in recurrence intervals is less than 0.3). The total static stress perturbation from close-by earthquakes, however, does not seem to strongly influence RES regularity. The uneven distribution of stress changes in time has a modest but significant impact on recurrence intervals. A significant reduction of recurrence intervals occurs in the case of very high-stress changes from neighboring events. Close-by events influence RES timing in a matter of several days or less by short-term triggering. Events that occurred within less than 1 day of an RES often imposed or experienced high-stress changes. A static stress increment of ~30 kPa can be enough to produce such short-term triggering. We find that the triggered repeating events are often near the end of their average earthquake cycle, but some events occur following a substantially shortened interval. When comparing the accelerated occurrence at the time of RES events following neighboring events with varying magnitudes, we find that the distance of short-term triggering increases from <1 km to 4 km for M1 to M4 events.

Citation: Chen, K. H., R. Bürgmann, and R. M. Nadeau (2013), Do earthquakes talk to each other? Triggering and interaction of repeating sequences at Parkfield, *J. Geophys. Res. Solid Earth*, *118*, 165–182, doi:10.1029/2012JB009486.

1. Introduction

[2] What determines the timing of earthquake recurrences and their degree of regularity is of fundamental importance to understanding the earthquake cycle and has important implications for earthquake hazard estimates. Previous studies have found that fault interaction may explain the temporal clustering and sequential occurrence of earthquakes or the delay of events in so-called stress shadows [e.g., *Harris*, 1998; *Toda et al*., 2012]. Of particular interest is whether or not fault interaction, that is, the advance or delay of a pending earthquake due to stress changes from nearby events, plays a first-order role in producing the apparent variability of earthquake recurrence intervals [*Stein*, 2003; *Freed*, 2005]. In addition to static stress interactions, the observation of remote triggering from distant earthquakes suggests a role of dynamic stresses in earthquake occurrence as well [e.g., *Hill et al*., 1993; *Velasco et al*., 2008; *Taira et al*., 2009]. There is substantial disagreement as to the degree to which near-field triggering is dominated by enduring static or transient dynamic stress changes [*Felzer and Brodsky*, 2006; *Parsons and Velasco*, 2009; *Richards-Dinger et al*., 2010]. To understand the role of fault interaction in the variability of earthquake recurrence intervals, one needs statistically sufficient observations of recurring earthquakes in a natural fault system. The relatively small amount of historical or paleoseismic data of recurring large earthquakes have provided only limited information about the degree to which stress interactions between earthquakes may influence earthquake recurrence intervals [e.g., *Sykes and Menke*, 2006].

[3] A characteristic repeating earthquake sequence (RES) is defined as a group of events with nearly identical waveforms, locations, and magnitudes that represent repeated ruptures of effectively the same patch of fault [e.g., *Nadeau and Johnson*, 1998]. Modeling studies and laboratory experiments have suggested that to drive the repeating ruptures, aseismic creep on the surrounding fault surface is required

[1]Department of Earth Sciences, National Taiwan Normal University, Taipei, Taiwan.
[2]Department of Earth and Planetary Science, University of California, Berkeley, California, USA.
[3]Berkeley Seismological Laboratory, University of California, Berkeley, California, USA.

Corresponding author: K. H. Chen, Department of Earth Sciences, National Taiwan Normal University, No. 88, Sec. 4, Tingzhou Road, Wenshan District, Taipei 11677, Taiwan. (katepili@gmail.com)

2169-9313/13/2012JB009486

[*Sammis et al*., 1999; *Anooshehpoor and Brune*, 2001; *Beeler et al*., 2001; *Johnson and Nadeau*, 2002]. The considerable evidence of RES observations on creeping fault segments from diverse tectonic settings also implies that aseismic slip at depth loads the repeating ruptures [*Vidale et al*., 1994; *Nadeau et al*., 1995; *Nadeau and McEvilly*, 1999; *Bürgmann et al*., 2000; *Matsuzawa et al*., 2002; *Igarashi et al*., 2003; *Uchida et al*., 2003; *Nadeau and McEvilly*, 2004; *Peng and Ben-Zion*, 2005; *Chen et al*., 2008]. From laboratory experiments [*Dieterich*, 1972; *Beeler et al*., 1994, *Marone*, 1998] and repeating earthquake observations [*Vidale et al*., 1994; *Nadeau and Johnson*, 1998], the recurrence interval is generally a function of seismic moment with larger seismic moment leading to longer stationary contact time. When compared among different fault zones, the average recurrence intervals of RESs also appear to be strongly controlled by the regional loading rate and distribution of creep on a fault [e.g., *Chen et al*., 2007].

[4] Earthquake predictability generally relates to the regularity of recurrence time. Recurrences of large repeating earthquakes tend to be more regular on relatively straight and isolated plate boundary faults of the subduction and transform type [*Sykes and Menke*, 2006; *Berryman et al*., 2012], while they are found to be highly variable due to nearby earthquakes, changes in strain rate, time-dependent variation in the frictional strength of fault, or other effects such as fluid pressure variations [e.g., *Lay and Kanamori*, 1980; *Sleep and Blanpied*, 1994; *Vidale et al*., 1994; *Ellsworth*, 1995; *Marone et al*., 1995; *Nadeau et al*., 1995; *Schaff et al*., 1998; *Ellsworth et al*., 1999; *Igarashi et al*., 2003; *Uchida et al*., 2003; *Nadeau and McEvilly*, 2004; *Taira et al*., 2009]. For example, RES near the 1989 M6.9 Loma Prieta and 1984 M6.2 Morgan Hill events reveal a significant reduction in recurrence interval at the time of the main shocks and subsequent increase in interval length, which follows the characteristic $1/t$ decay of Omori's law [*Schaff et al*., 1998; *Peng et al*., 2005]. The RES recurrences directly reflect decaying afterslip adjacent to a main-shock rupture [e.g., *Nadeau and McEvilly*, 2004; *Templeton et al*., 2009]. Similar accelerations were observed following the 2004 Parkfield earthquake [*Lengline and Marsan*, 2009; *Chen et al*., 2010b].

[5] Several unsolved problems regarding the recurrence properties of natural earthquake sequences remain, however: How do the repeating sequences respond to static stress perturbations associated with nearby earthquakes? To what degree does earthquake interaction influence the timing of repeating earthquakes? And finally, do spatially adjacent repeating sequences communicate with each other in a way that is observable in the relative occurrence times of their events? These questions cannot be adequately answered without documentation of a statistically significant dataset of recurrence properties from naturally occurring earthquake populations.

[6] The detailed record of microearthquake data from the borehole High-Resolution Seismic Network (HRSN) and surface Northern California Seismic Network (NCSN) at Parkfield, California provides a unique opportunity to examine how earthquake interaction acts on the observed recurrences of the repeating events. We consider a subset of data from a catalog of 216 RESs with events ranging from $M = -0.4$ to $M = 3$ containing a total of 1076 recurrence intervals to study their recurrence behaviors in space and time. Taking advantage of this large number of repeating microearthquakes with precisely determined relative locations, we analyze the repeating-event catalog for empirical evidence of interaction and then offer a conceptual model for the mechanics of such interaction. We also consider the role of nonrepeating background seismicity relying on a relocated catalog of 5724 M0.2–5.0 events that occurred during the 1984–2004 period [*Thurber et al*., 2006]. We estimate stress changes from all nearby RESs and background events in the study area to evaluate the degree of static earthquake interaction and triggering.

2. Repeating Earthquakes at Parkfield

[7] Microearthquake data collected by the NCSN and HRSN were used to search for repeating earthquakes at Parkfield using measures of waveform similarity (i.e., maximum cross-correlation and phase and amplitude spectral coherence) between event pairs at all operating network stations [*Nadeau et al*., 1995; *Nadeau et al*., 2004]. Event clusters (i.e., "cluster subgroups" in *Nadeau et al*. [1995]) that have essentially common locations and waveforms are grouped into 216 RESs composed of 1292 events and 1076 recurrence intervals. The magnitudes of events within each RES typically vary by less than ± 0.1 magnitude unit [*Nadeau and Johnson*, 1998], and sequence magnitudes range between 1.3 to 3.0 for the NCSN recorded events and -0.4 to 1.67 for the borehole HRSN events.

[8] At Parkfield, the surface NCSN has reliably located earthquakes to less than the M1 level since 1984, primarily relying on short-period surface seismometers. During the period 1984–2004 ending before the September 28 Parkfield M6 main shock, 30 M1.3~3.0 NCSN-derived repeating sequences were identified with a total of 178 events, yielding 148 recurrence intervals in a range of 0.65 to 10.66 years [*Nadeau and McEvilly*, 2004]. The individual NCSN repeating sequences are composed of from 2 to 15 events and have average recurrence intervals ranging from 1.23 to 8.73 years.

[9] The higher detection sensitivity of the borehole HRSN has revealed a large number of additional repeating microearthquake sequences ranging in magnitude from -0.4 to +1.67 [*Nadeau et al*., 1995; *Nadeau and McEvilly*, 1997]. Recording by the HRSN deep borehole sensors began in early 1987, but the original data acquisition system failed at the end of June 1998. In 2001, the HRSN network was upgraded, and three new borehole stations were installed to improve resolution of the structure, kinematics, and monitoring capabilities in the San Andreas Fault Observatory at Depth drill-path and target zone [*Nadeau et al*., 2004]; in late July of that year, the upgraded and expanded HRSN once again began reliably recording the very small microearthquakes. Because smaller magnitude RESs are more numerous and repeat more frequently, the HRSN RES catalog significantly increases the amount of repeating-event data available for analysis and provides a better opportunity to examine recurrence properties. During the 1987–1998 operational period of the HRSN, 186 repeating sequences were identified with each sequence composed of 2 to 19 events. The total number of 1114 unique events results in 928 recurrence intervals that range from 0.005 to 6.95 years, while the average recurrence interval of each sequence ranges from 0.57 to 4.46 years. Figure 1a shows the catalog locations of

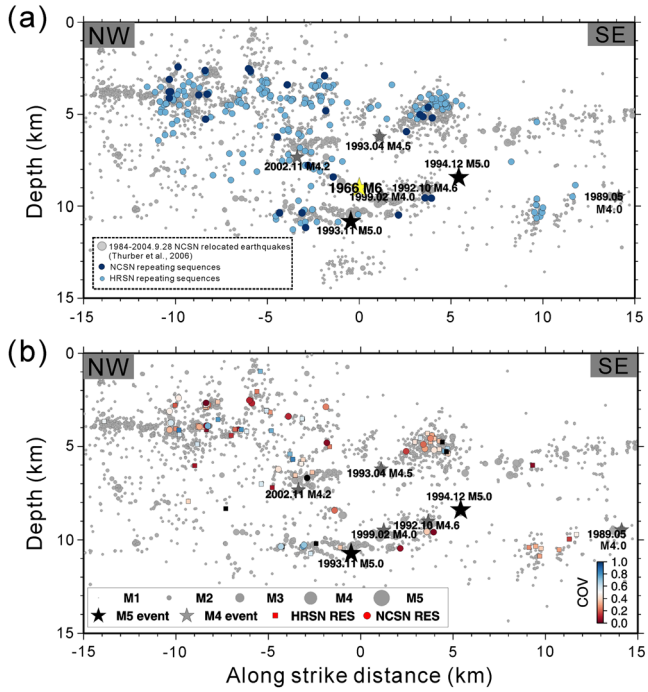

Figure 1. (a) Along-fault depth section of the distribution of 30 NCSN (1984–2004, dark blue circles) and 186 HRSN (1987–1998, blue circles) RES shown at their average original catalog locations with the symbol size exaggerated. Relocated background seismicity (1984–2004) is denoted by gray filled circles scaled by event magnitude [*Thurber et al*., 2006]. For reference, the 1966 *M*6 hypocenter is shown by a yellow star. The hypocenter of the 2004 *M*6 Parkfield earthquake is located at 21 km distance. (b) The same cross section showing precisely relocated background seismicity (gray circles, *Thurber et al*. [2006]) and the 30 NCSN-derived (colorful circles) and 82 HRSN-derived RES (colorful squares) at their average precisely relocated catalog locations. Fill colors are keyed to the COV in recurrence interval. Seven sequences with only two events (COV = 0) are shown by black circles and squares. Labeled gray stars indicate *M*4–5 events. The reference point (0, 0) is at latitude 35.955°N and longitude 120.495°W with the orientation of N45°W.

all 216 NCSN and HRSN RESs shown by dark blue and light blue circles, respectively, together with the precisely relocated catalog from *Thurber et al*. [2006].

[10] To have a consistent set of locations for our analysis of stress interactions, we identified sequences having at least one event in common with the double-difference (DD) earthquake location catalog of NCSN events in the Parkfield area [*Thurber et al*., 2006] and replaced our original RES-event locations with those from the DD catalog when they existed. Many of the smaller magnitude RES events from the HRSN catalog do not have locations in the NCSN-based DD catalog due to the greater completeness of HRSN event detection. If an HRSN-identified RES has no event in the DD catalog, the RES is excluded from further analysis. If an HRSN RES has at least one event in the DD catalog, then the average of available DD locations for the RES events is used as the location for any events in the RES that were missing DD locations. The DD locations for events in the NCSN RESs differ between 16 m and 427 m, with 73% of the events found to lie within 100 m of each other. Compared to location differences of a few kilometers in the NCSN original catalog, the distribution of RES DD locations provides an estimate of the relative location uncertainties of nearby events. The resulting integrated catalog of RESs with precise relative locations contains 30 NCSN (178 events) and 82 HRSN (477 events) RESs ranging in average RES magnitude from 0.34 to 3.0. We note that although this integration has reduced the number of RESs by ~50%, it provides a consistent, high-resolution spatial framework for analysis of the RESs and nonrepeating background events.

[11] The relocated 112 RESs, including 30 NCSN (1984–2004, *M*1.34~3.0) and 82 HRSN (1987–1998, *M*0.34~1.67) sequences containing 655 events, are shown in Figure 1b. Seven RESs that contain only two events each are shown by black circles (NCSN) and squares (HRSN). Eighty-seven sequences have four or more recurrence intervals. More than 80% of the RESs are located at shallow depths above 7 km where most of the background seismicity (either not repeating or not yet identified as repeating) is found as well. Table 1 details the numbers of RES in the original and integrated NCSN and HRSN catalogs.

3. Controls of RES's Regularity and Recurrence Interval

3.1. Number of Nearby Events

[12] If earthquake interaction is responsible for some of the variability of earthquake recurrence intervals (hereafter referred to as "*Tr*"), earthquakes that are more isolated from

Table 1. Data Number of Repeating Earthquakes

	1984.221–2005.105	1987.136–1998.179	1984.222–2004.272	1987.136–1998.179	1984.222–2004.272
	NCSN (original)	HRSN (original)	NCSN (integrated)	HRSN (integrated)	NCSN + HRSN (combined)
Magnitude range	1.0~3.0	−0.4~1.67	1.34~3.0	0.34~1.67	0.34~3.0
RES	30	186	30	82	112
RES with N* ≥ 2	29	169	29	76	105
RES pairs (N = 1, COV = 0)	1	17	1	6	7
event number	218	1114	178	477	655
event number with N ≥ 2	216	1080	176	465	641
Tr number	188	928	148	395	543
Tr number with N ≥ 2	187	911	147	389	536

*N is number of recurrence intervals *Tr* in an RES.

neighboring events might be expected to recur more regularly. To assess how recurrence interval variability relates to the activity of nearby earthquakes, the locations of RESs with varying coefficients of variation in *Tr* (COV) are shown in Figure 1b. The COV for a given sequence is the standard deviation of the recurrence intervals divided by their mean:

$$COV = \frac{\sqrt{\sum_{i=1}^{N} \left(Tr_i - \overline{Tr}\right)^2 / N}}{\overline{Tr},} \quad (1)$$

where $\overline{Tr}$ is the mean duration, and N is the number of the recurrence intervals in a sequence, respectively. Under stationary conditions, a COV of 0 reflects perfect periodicity, COV $\sim$ 1 is compatible with a Poissonian distribution, and COV $>$ 1 indicates temporal clustering. For natural repeating earthquakes, COV is found to be ~0.5 [*Ellsworth et al*., 1999], while earthquakes as a whole more closely follow a Poissonian distribution with COV of ~1 [*Ellsworth*, 1995]. The COV of each RES is denoted by color-coded circles and squares in Figure 1b. We note that the COV for the seven sequences with only two events shown by black symbols in Figure 1b (COV = 0) are excluded from the analysis below, leaving 105 RESs.

[13] As indicated by the histogram of COV in Figure 2a, we find that 36% of the RESs are characterized by a COV $\leq$ 0.3. These quasi-periodic sequences span a magnitude range of *M*0.7~2.8 and are mostly located at shallow depths, away from the rupture zones of several historic M $>$ 4 events that are mostly located deeper than 6 km [*Chen et al*., 2010a]. From visual inspection, however, there is no simple relationship between spatial isolation and periodicity of RESs (i.e., COV $<$ 0.3 RESs near *M*4 events in Figure 1b). To understand if spatial variations in the COV are related to the apparent isolation from other events, we plot the number of 1984– 2004 earthquakes that occurred within 5 km from the 105 RESs against their COVs in Figure 2b. The RESs with small COV ($\leq$0.2) generally have a smaller number of neighboring events. If we repeat this analysis for distances of 1 km and 5 km, the distribution remains similar. This trend seems to be clearer when only the neighboring earthquakes with greater magnitude than the respective RES are counted (Figure 2c). To confirm that the observed COV distribution indicates a significant relationship with the number of nearby events, we compare the observed COV distribution with values derived from randomly resampled recurrence intervals (10 runs in total) as shown by gray lines in Figures 2b–2d. In the range of COV $<$ 0.3, we find that the behavior of a randomly drawn COV population does not show a clear distinction from the observed distribution (gray and black lines in Figure 2c). This suggests that the interaction with numerous close-by background earthquakes may not be the only factor that perturbs the regularity of RES.

3.2. Role of Total Stress Perturbation From Nearby Events

[14] To explore how static stress changes imposed by neighbors affect the timing of RES events, seismic moment and stress change are taken into account. Here we introduce a simple expression for the static shear stress change (*dS*)

$$dS = 1/6\pi M_0/r^3 \quad [Aki\ and\ Richards, 1980], \quad (2)$$

where r is the distance from an RES to the hypocenter of each neighboring event (with seismic moment M_0) on a single fault plane assuming a strike of N40°W. Empirical tests using the shear stress change calculated from an elastic dislocation model [*Okada*, 1992] produce consistent values of in-plane stress changes with equation (2). In this calculation, we assume that all earthquakes lie on a single plane and thus increase stress on their neighbors, which is clearly not always the case (e.g., precise earthquake relocation indicates two fault strands that are ~0.3 km apart at shallow depth and merge below ~5 km [*Nadeau et al*., 2004; *Waldhauser et al*., 2004]). The COV of the 105 RES is plotted versus the cumulative stress perturbation from nearby events in Figure 2d, where the *dS* value for individual events determined from equation (2) is capped at 1 MPa to avoid the cumulative stress values to be dominated by the extreme stress changes obtained for very close-by neighbors (several 10s of meters). We see no systematic relationship between COV and the estimated cumulative stress perturbation an RES experiences from neighboring events. The calculated cumulative stress perturbations are highly variable with no distinction from a random distribution of COV values (gray lines in Figure 2d), suggesting that the total stress change due to nearby earthquakes cannot explain COV variation.

[15] We also notice that the cumulative stress perturbations are often dominated by the contribution from a number of very close, high-stress change events. It is therefore necessary to consider the contribution on each individual RES event. When stress perturbation on each individual RES event is considered as *dS*(*i*) in Figure 3a, the COV versus cumulative stress perturbation in Figure 3b shows no simple relation between RESs' regularity and stress perturbations on the RESs' recurrence intervals. However, more regular events (COV $<$ 0.2) appear to be made up predominantly

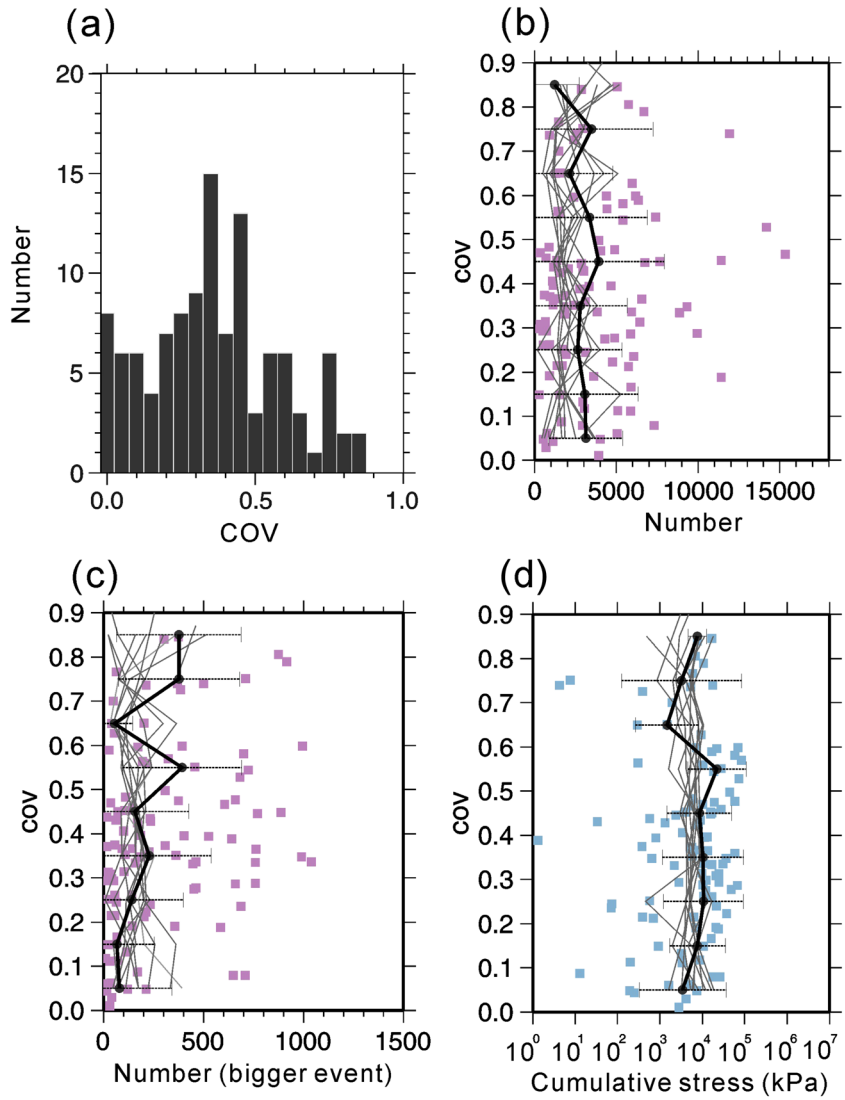

Figure 2. (a) Histogram of COV values of the 112 RESs. (b) Number of all neighboring earthquakes from 1984 to 2004 within a distance of 5 km versus COV in recurrence interval of the 105 RESs without sequences with two events (COV = 0.0). (c) Number of neighboring earthquakes of equal or larger magnitude than the sequence events within 5 km versus COV in recurrence interval of the 105 RES. (d) Cumulative shear stress change at each RES location from all neighboring earthquakes versus COV in recurrence interval. Stress-change values from individual events were capped at 1 MPa. In each plot, the median of earthquake number (Figures 2b and 2c) and cumulative stress change (Figure 2d) in each 0.1 COV interval is denoted by black circles connected by black lines. Horizontal bars indicate the standard deviation of the values in each bin. Synthetic data generated by 10 sets of randomly resampled recurrence times is shown in gray lines for median values.

of greater magnitude (circles in warm color below COV = 0.2 in Figure 3b). This is consistent with the observed COV distribution shown in Figure 2c that the relative magnitude may play a role on the degree of stress interaction.

3.3. Stress Perturbation From Nearby Events During a Recurrence Interval

[16] How is the uneven distribution of the stress changes in time affecting the variability of recurrence intervals? If static stress interactions influence the timing of earthquakes, we expect that events will occur more rapidly after and during periods of greater external load increases. Thus, we explore whether the static stress change experienced by an RES during a given recurrence interval correlates with the length of that interval. Here, the time spanned by a recurrence interval is normalized by the average recurrence interval for the respective sequence and plotted against the external stress changes taking place during that period. We again cap the stress increment from an individual event at 1 MPa. In Figure 3, we consider normalized *Tr* versus cumulative stress change (*dS*) and stress change rate (*dS*/*Tr*) in the preceding interval, considering effects from nearby events (within 5 km) during that period. Figure 3c shows that short intervals (small normalized *Tr*) do not systematically correlate with

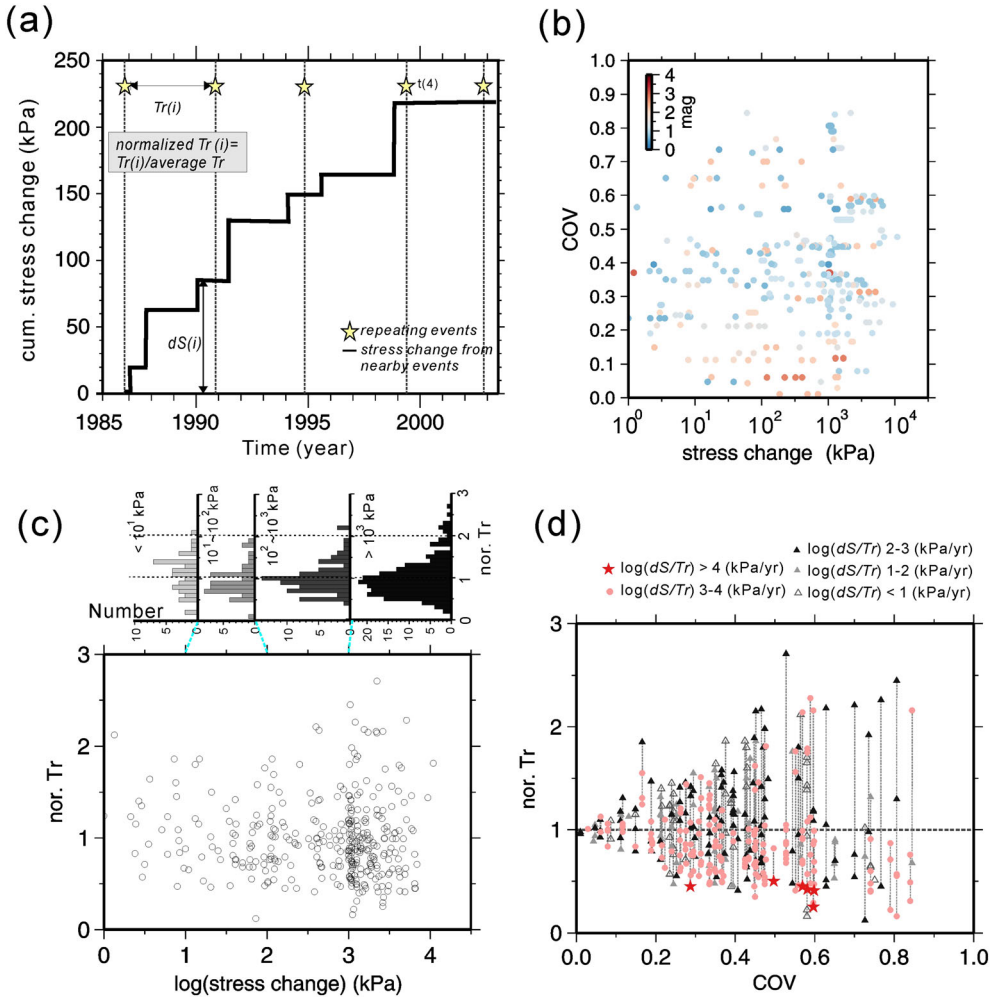

Figure 3. (a) Schematic time distribution of cumulative stress change from nearby earthquakes showing how the stress changes $dS(i)$ and normalized Tr ($Tr(i)$/average Tr) are calculated. Yellow stars indicate the repeating events' occurrence times. Black line indicates the cumulative stress change from all earthquakes within 5 km of an individual RES. (b) COV against the stress change ($dS(i)$) each RES event experienced during the preceding recurrence interval. (c) (Lower panel) Normalized Tr of all RES events as a function of stress change stressing rate ($dS(i)$) during the preceding recurrence interval. (Upper panel) Histograms of normalized recurrence intervals for different stress change ranges. (d) Normalized Tr values versus COV of each RES. The RES events exposed to different ranges of stressing rates are shown by different symbols. Red stars, pink circles, black triangles, gray triangles, and open triangles indicate the log stressing rate of $dS(i)$ >4, 3–4, 2–3, 1–2, and <1 kPa/yr, respectively. Vertical dashed line connects the data points belonging to the same sequence.

higher static stress changes during that interval. The upper panel of Figure 3c illustrates the distribution of normalized Tr values exposed to varying stress ranges. If the stress change experienced during a recurrence interval does not notably influence the duration of the interval, the RES would have a peak around normalized $Tr = 1$. The population of RES that experienced stress change greater than 1 MPa have a mean normalized recurrence interval of 0.89 (median value = 0.86). The remaining RES events preceded by periods with stress change less than 1 MPa have a mean normalized Tr of 1.01 (median value 0.97), and the mean and median Tr for events that experienced <10 kPa is 1.09, suggesting a modest but significant reduction of recurrence intervals by high-stress changes. To see if high-stress events are leading to short Tr, we also highlight the RES events exposed to particularly high-stress changes with red stars and pink circles in Figure 3d, whereas vertical dashed line connects data points belonging to the same sequence. Note that the increasing COV reflects the spread of Tr for a given sequence. Events that experienced peak stress changes (>10 MPa/year) have particularly low normalized Tr (<0.6), suggesting a substantial shortening of a recurrence interval by extreme stress perturbations.

4. Controls of RES Events' Timing

4.1. Space-Time Relationship With Nearby Seismicity

[17] We further examine how much the repeating earthquake timing can be explained as a result of triggering from nearby seismicity by considering the relative times of individual events. For each RES event, the time difference (DT)

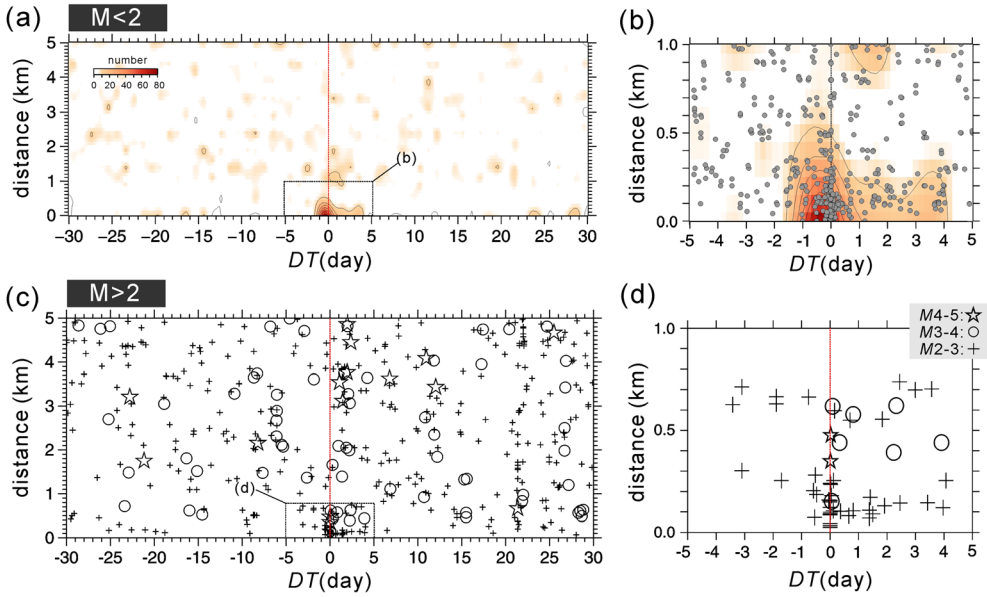

Figure 4. (a) Separation distance versus time difference between RES events and nearby $M < 2$ earthquakes. Positive/negative DT values correspond to the times of preshocks/postshocks that occurred before the RES events. The number of $M < 2$ events in each 1 day × 0.25 km grid box is denoted by color and contour lines (10 event intervals). (b) Close-up map view of dashed box in Figure4a for <5 km and ≤1 day. Gray dots indicate the individual $M < 2$ events. (c) Separation distance versus time difference between RES events and nearby M4~5 (stars), $3 \leqq M < 4$ (circles), and $2 \leqq M < 3$ (crosses). (d) Close-up map view of dashed box in (c) for <5 km and ≤1 day.

with all other earthquakes within a distance of 5 km is considered, together with the stress change induced by preceding neighboring events (preshocks) and vice versa for events following the RES events (postshocks). The close-by background events across a range of $M < 2$ to $M5$ are selected to show their space-time relationship with the RES in Figure 4. A large number of $M < 2$ events (Figures 4a and 4b) and $M2$–3 events (crosses in Figures 4c and 4d) occur very close in space and time to the RES. In Figure 4, the concentration of events appears in the <1 day and <5 km area, with 290 and 303 preshocks and postshocks, respectively (Table 2). This suggests that during $|DT| \leq 1$ day, small earthquakes often trigger others over short distances. A larger number of $M > 3$ events are found to have occurred shortly before the RES (circles and stars in Figure 4c). There are 24 $M > 3$ preshocks versus four $M > 3$ postshocks within 5 days of the RES events, showing that some of the RES events were triggered by these larger earthquakes, which occurred across the range of distances considered. The $M > 3$ events seem to have a wider triggering distance and longer triggering time compared with $M2$, and the smaller RES events often occur during the aftershock sequence of preceding larger events. We will carefully examine the magnitude dependency of triggering behavior in session 5.1.

[18] Given the short distance between events in Figure 4, one may argue if some background earthquakes actually belong to a RES, and so the observed triggering is by an event of the same repeating sequences. With waveform based selection criteria for repeating earthquake identification, however, it is unlikely for a close-by event with identical waveform to be ignored. It is still possible that members of a RES are incorrectly classified as nonmembers if their waveforms overlap with those of other events occurring within a few seconds on the same patch or other locations. In the Parkfield area, this phenomena is rare, occurring <1% of the time, which implies that the probability of triggering of a repeating sequence by missed events from the same sequence is small and will have little effect on our overall conclusions.

4.2. Static Stress Perturbation From Nearby Seismicity

[19] To see how much the event times can be explained by stress perturbation from nearby earthquakes and what stress increments are needed to produce effectively immediate triggering, the stress changes are then computed. We use the moment of RES events and background events in the stress calculation (equation (2)) for the postshocks ($DT < 0$) and preshocks ($DT > 0$), respectively. When stress changes induced by nearby events are computed for varying DT ranges, we find that a larger number of high-stress change events (>1 kPa) occur during $|DT| \leq 5$ days (see Figure S1 in the auxiliary material).[1] A distinct difference between $|DT| \leq 5$ and >5 days histograms appears at >1 kPa, as denoted by the gray-shaded area in Figure S1. Therefore, the cutoff stress change is selected to be 1 kPa for the following short-term

Table 2. Number of Preshocks and Postshocks within 5 km of 655 RES Events

Number	30–300 days	In 30 days	In 5 days	In 1 day	In 5000 s	In 1000 s
Preshock	17,892	3,804	904	290	86	41
Postshock	20,594	3,749	852	303	105	60
>1 kPa preshock	425	338	198	136	65	36
>1 kPa postshock	430	281	166	140	74	48

Table 3. Occurrence Rate (Events per Day) of Preshocks and Postshocks Within 5 km of 655 RES Events

Rate (#/day)	30–300 days	In 30 days	In 5 days	In 1 day	In 5000 s	In 1000 s
Preshock	66.3	126.8	180.8	290.0	1486.1	3542.4
Postshock	76.3	125.0	170.4	303.0	1814.4	5184.0
>1 kPa preshock	1.6	11.3	39.6	136.0	1123.2	3110.4
>1 kPa postshock	1.6	9.4	33.2	140.0	1278.7	4147.2

triggering analyses. Tables 2 and 3 summarize the number and rates of earthquakes within 5 km distance for a number of *DT* ranging from less than 1000 s to 30–300 days, including both total event numbers and those that experienced

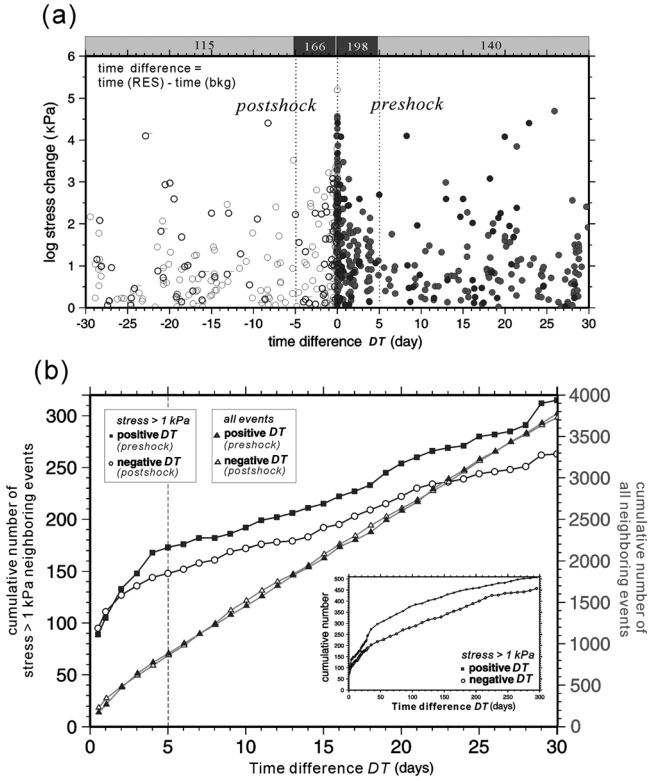

Figure 5. (a) Static stress change as a function of time difference between repeating events and nearby background earthquakes (bkg) within 5 km distance. Stress changes computed in the postshock case are those imposed by the RES on the subsequent events, whereas in the preshock case the stress changes are those imposed on the RES event. The labels in the upper panel indicate the number of nearby events with stress changes >1 kPa within 5 days and 5–30 days following/preceding the RES shown by circles. The total number of preshocks and postshocks within 30 days and 5 km from all RES events (without considering their stress change) are 3804 and 3749, respectively. (b) Cumulative number of all background events with increasing time difference *DT* from RES events for preshocks and postshocks (solid and open triangles). The measures for the events with higher stress changes (>1 kPa) are shown by filled squares and open circles for preshocks and postshocks, respectively. Inset shows the >1 kPa event numbers for the *DT* range out to 300 days.

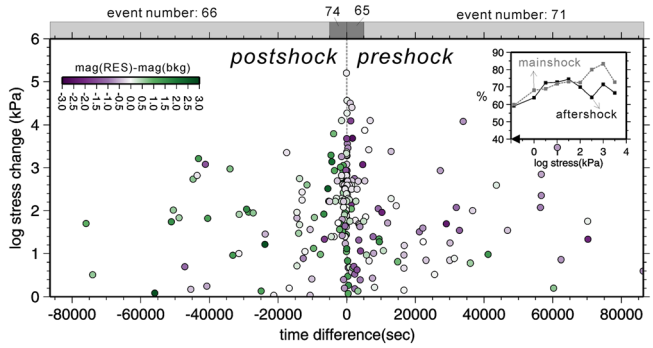

Figure 6. Close-up of data in Figure 5a for static stress changes >1 kPa and time differences shorter than 24 h (86,400 s) from the time of the 655 RES events considered. Background events are color coded by magnitude difference with the associated RES event. Green-colored postshocks (preshocks) are aftershocks (foreshocks) of the associated RES, while purple-colored postshocks (preshocks) are larger than the preceding (following) RES. The values in the upper panel indicate the number of nearby events during 5000 s to 1 day and within 5000 s following/preceding the RES with static stress changes >1 kPa. The inset shows data percentage of varying stress-level populations for time differences shorter than 1 day from the RES events. Preshock events with greater magnitude than RES are labeled as main shock, while postshocks with smaller magnitude than RES are aftershocks. For example, 64% of the >1 kPa postshocks are aftershocks, while 68% >1 kPa preshocks are main shocks.

or imposed stress changes greater than 1 kPa. For example, within 1 month preceding and following the 655 RES events, the total number of preshocks and postshocks within 5 km are 3804 and 3749, respectively. Out of this population of 7553 events, 338 (281) preshocks (postshocks) imposed (experienced) stress changes greater than 1 kPa. When stress changes induced by nearby events are computed for varying *DT* ranges, we find that a larger number of high-stress change events ($dS > 1$ kPa) occur during $|DT| \leq 30$ days (Tables 2 and 3). In Figure 5a, we plot stress changes for $|DT| \leq 30$ days and $dS > 1$ kPa for preshocks and postshocks showing clear evidence of short-term triggering by and of very close-by, high-stress events. As illustrated by denser population in Figure 5a, the short-term triggering is more evident in 5 days. The approximately >1 kPa preshocks are much more frequent within 5 days preceding the RES (solid line with filled squares in Figure 5b). High-stress event rates continue to greatly increase with decreasing time windows about the time of the RES. As shown in Figure 6, 50% and 30% of the $|DT| <$ 1 day, $dS > 1$ kPa events are confined to within 5000 s and 1000 s of the RES event, respectively. Events that occurred within less than 1 day of an RES often imposed or experienced particularly high-stress changes.

[20] Rates of nearby preshocks and postshocks systematically increase with decreasing time before and after an event, and this increase is most pronounced for events that imposed or experienced higher stress changes (Figure 5a). Compared to a preshock rate of 66.3 events/day during the interval of 30 to 300 days before the RES events, we find 180.8 events/day during the last 5 days (Table 3). A plot of cumulative number of all events, independent of stress change, versus increasing $|DT|$ (triangles in Figure 5b) shows

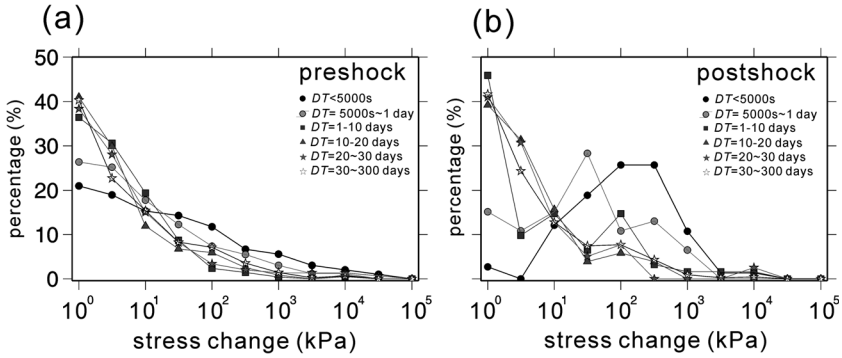

Figure 7. (a) Percentage of preshock events inducing stress increases for a range *DT*. By only considering events >1 kPa, plotted values give percentage of preshocks with the calculated stress changes on horizontal axis by $10^{0.5}$ stress interval. (b) Percentage of postshocks versus stress increases by nearby RES events.

relatively modest changes in occurrence rate as a function of time difference from the potential trigger event, except for a larger number of events within 1 day. However, a remarkable difference between the number of preshocks and postshocks close in time to an RES event appears if only events with higher stress change are considered, as illustrated by plotting the cumulative number of events with >1 kPa stress change versus increasing |*DT*| in Figure 5b. The rate of >1 kPa postshocks do not show quite as much change with time following the RES (solid line with open circle in Figure 5b) as do the high-stress preshocks. Given that the events used to determine stress changes in the preshock and postshock domain are background seismicity and repeating events, respectively, and repeating events are on average of smaller magnitude, the larger number of higher-stress-change preshocks is to be expected. Beyond the 5 day time window, both >1 kPa preshocks and postshocks exhibit similar occurrence rates, as shown by the similar slopes of the solid lines in Figure 5b. The event rates of high-stress preshocks and postshocks reveal systematic decreases out to 300 days (Figure 5b inset, Table 3). Tables 2 and 3 show that the frequency of all events and of events with stress increases >1 kPa within the 30-day period considered in Figures 4 and 5 is substantially greater than over longer time periods spanning 30–300 days away from the times of RES events.

[21] As the time window about the RES events we consider gets shorter, the relative contribution of very high-stress change events increases. This is further illustrated in Figure 7, where the number of events in the varying *DT* window (<5000 s, 5000 s to 1 day, 1–10 days, 10–20 days, 20–30 days, and 30–300 days) imposing a range of stress changes (in log stress increments of 0.5 kPa) is divided by the total number of >1 kPa events. In Figure 7a, these data percentages are plotted against the stress change ranges imposed on a subsequent RES for each *DT* window. The percentage of high-stress change preshocks is the greatest for the $DT < 5000$ s window (black circles), with declining percentages for longer *DT* intervals. For example, 29 out of 219 (~12%) >1 kPa preshocks in the $DT < 5000$ s window impose stress changes of log stress = 2 kPa (for the range of 10^2–$10^{2.5}$ kPa) on an impending RES event, while only five out of 206 events (~2%) fall in that stress-change range in the *DT* = 1–10 day window. Note that the shorter than 1 day *DT* events start to have the highest percentage at log stress = 1.5 kPa (~30 kPa). The postshock results in Figure 7b show a similar pattern where a greater data percentage in high-stress change appears in the $DT < 1$ day triggering windows, and the $DT < 1$ day events start to dominate at ~30 kPa as well. This confirms that the higher the imposed stress changes are, the shorter the time to the eventual occurrence of a triggered event gets.

4.3. Role of Earthquake Magnitude

[22] How does the triggering effect vary with the relative magnitude of the trigger and triggered events, or put in other words, are triggered events aftershocks or main shocks of preceding events? When considering the >1 kPa events, we find that 68% of preshocks occurring within 1 day have a greater magnitude than the following RES events (purple-colored preshocks in Figure 6), whereas 64% of postshocks have smaller magnitudes than the preceding RES events. Here we consider the preshocks with greater magnitude than the subsequent RES as "main shock," while the postshocks with smaller magnitude are "aftershocks." When considering all 290 preshocks and 303 postshocks independent of the stress change involved within 5 km and 1 day of the 655 RES events, 60% of preshocks are found to represent main shocks, and 59% of postshocks are aftershocks. Within 5000 s, there were a total of 86 and 105 preshocks and postshocks. The percentage of main shocks and aftershocks increases with increasing stress level as illustrated in the inset of Figure 6. More than 85% of RES events that are triggered by stress changes of greater than 1 MPa are aftershocks of larger preshocks. Thus, short-term triggering often involves greater-magnitude earthquakes that act as main shocks and facilitate the occurrence of nearby aftershocks including the RES events. Smaller events can act as foreshocks if they are nearby and produce large stress changes.

5. Relation of RES Triggering and Their Earthquake Cycle

5.1. Wider Triggering Distance for Bigger Preshocks?

[23] The triggering periods by preshocks we document in section 4 are short compared to the recurrence intervals of

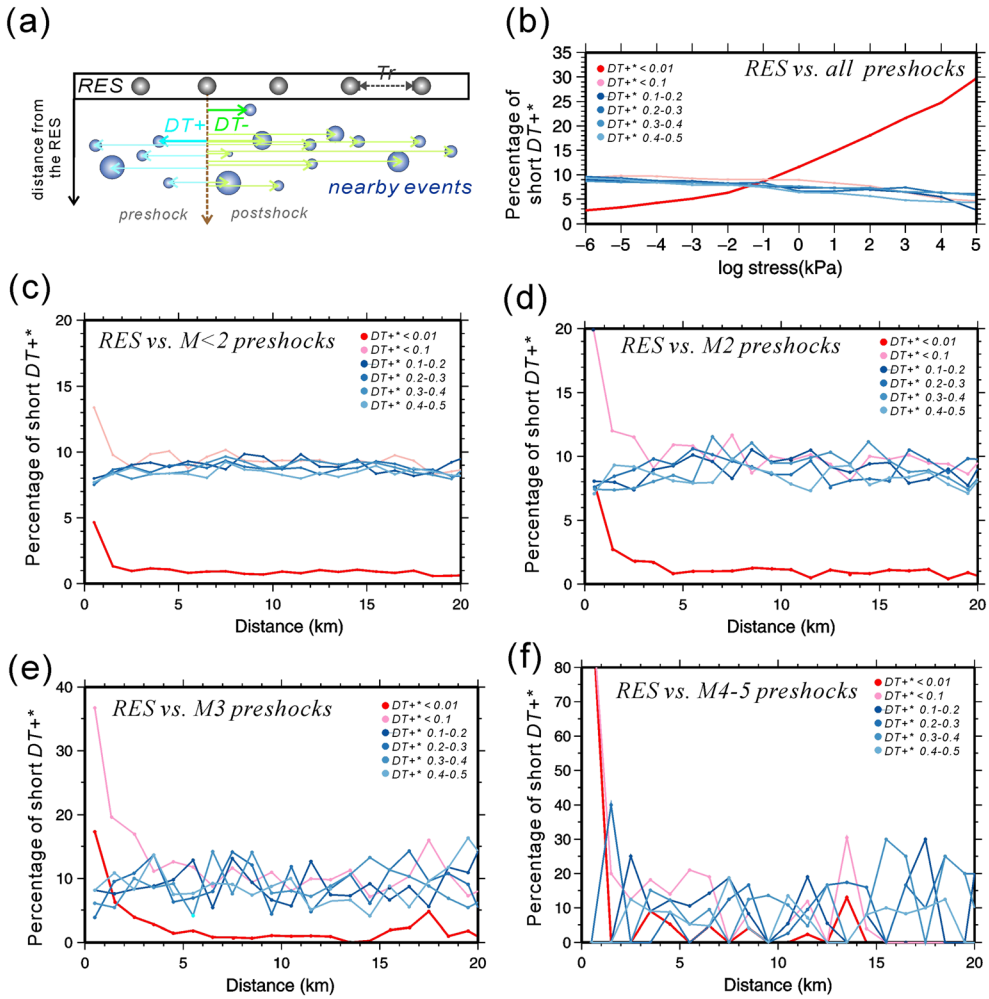

Figure 8. (a) Schematic illustration of the relative time of RES occurrences with respect to a nearby event with varying spatial distance. Each RES paired with a nearby event provides either *DT*+ or *DT*− measurements. (b) Percentage of short normalized *DT*+* ranges (*DT*+ divided by the average recurrence interval of a given RES) as a function of stress change. Percentage of *DT*+* as a function of distance between preshocks and RES event for (c) $M < 2$, (d) $2 \leqq M < 3$ events, (e) $3 \leqq M < 4$, and (f) $M \geqq 4$ preshocks.

the RES events involved. To directly relate the trigger times of RES events to the length of the RES recurrence intervals, we divide the preshock *DT*+ (hereafter we use *DT*+ and *DT*− to present the preshock and postshock *DT*, respectively) by the average recurrence interval of the respective RES to obtain *DT*+*, the fraction of an average recurrence interval spanned by *DT*+. In Figure 8, we display the same data as in Figure 7a but use the fractional *DT*+* ranges for the preshock – RES-event time spans. If background events were randomly distributed in time, each *DT*+* range would have a percentage value according to its fractional value (i.e., 10% for 0.1 *DT*+* intervals).

[24] The *DT*+* versus stress change in Figure 8b reveals that very short *DT*+* (<0.01) dominate the population of events that experienced high-stress changes, whereas the percentage does not change much with stress for *DT*+* >0.01. To see if separation distance is a proxy for stress level, we next plot *DT*+* as a function of distance for different magnitude ranges to explore the dependence of triggering distance on preshock event magnitude. The percentage of very short preshock *DT*+* (<0.1) is high in the near field compared with *DT*+* > 0.1 data and the value of 10% predicted for *DT** = 0.1 intervals drawn from a random population [*Chen et al.*, 2010a]. In Figures 8c–8e, we show that an accelerated occurrence of repeating events is evident to ~1 km, 1–2 km, and 3–4 km distance from the background events for *M*1, *M*2, and *M*3 events, respectively (*DT*+* <0.01 and 0.1). Fewer *M*4 events in our integrated catalog lead to poor resolution in fraction versus distance plot (Figure 8f); nevertheless, our earlier study of the complete HRSN repeating earthquake catalog reveals an influence distance of 4 km for the *M*4–5 source events [*Chen et al.*, 2010a]. The comparison of the influence zones for varying trigger-event magnitudes indicates wider triggering distances and longer triggering times for bigger preshocks, also evident in the distribution of events shown in Figure 4.

5.2. Are Triggered RES Events Late in Their Earthquake Cycle?

[25] We evaluate how preshocks influence the RES events' timing with respect to the RES earthquake cycle. For this analysis, we consider different measures of time difference

at+ and *at*−, as illustrated in Figure 9a. Here, *at*+ represents the time difference between a preshock and the subsequent RES event, and *at*+* is the fractional recurrence interval defined as *at*+ divided by the average recurrence interval of the RES. The absolute and fractional time differences *at*− and *at*−* are between the preshock and the most recent event in the RES. If the triggered RES events are already late in their repeating earthquake cycle, the fractional *at*+* of the RES would be small compared to the time between the most recent RES occurrence and the preshock and *at*−* would be close to 1. In Figure 9b, we divide the data space in the *at*−* versus *at*+* plot into four quadrants with the lines *at*+* + *at*−* = 1 and *at*−* = *at*+*. Quadrants A and B indicate regions where the sum of *at*+* and *at*−* (i.e., the recurrence interval spanning the reference preshock event) is longer than the average cycle, and data in quadrants B and C represent events that occurred in the second half of the recurrence interval.

[26] The percentage of data values in each quadrant is denoted by the number inside the quadrants in Figures 9c–9f. If the events are late in their earthquake cycle and terminate a smaller than average recurrence interval, then data would fall in quadrant C. For preshocks producing stress changes >1 kPa, we see a concentration of events at very low *at*+* values with *at*−* values near 1 (Figures 9d and 9e); that is, many short-term triggered events were close to or beyond the time of their average recurrence interval. More than half of the data points fall in quadrants B or C, showing *at*+* < *at*−* with that fraction increasing with the stress change imposed by the preshock on the RES location (from 52% for $dS < 1$ kPa to 64% for $dS > 1$ MPa). When we consider the preshocks that lead to *at*+ < 1 day in Figure 10, the concentration of *at*−* ~ 1 is visible. Distribution of *at*−* shows generally broad distributions about 1, independent of stress level. This suggests that higher stresses do not seem to produce a clear pattern of letting events recur prematurely (short *at*−*). We can further conclude that (1) strong stress increases from neighboring events cause many RES events to occur promptly (large number of very small *at*+*/*Dt* +* values as shown in Figures 8b and 9d–9f), (2) such stress triggered events can be close to the end of their average recurrence interval (*at*−* values near 1 in Figures 9d–9f), and (3) some RES events triggered by strong stress steps can be early in their cycle and thus lead to somewhat shortened recurrence intervals (Figures 9c, 9e, and 9f).

6. RES-Event Clusters and Interaction

[27] To see if triggered RES events are distributed uniformly in time during the study period, we investigate the temporal distribution of RES events that experienced higher than 1 kPa stress change from nearby preshocks and occurred within a short time interval ($DT < 30$ days). In Figure 11a, we find that the $DT < 30$ days events are clustered in time (lower panel), corresponding to high-stress changes (upper panel). There are several time-clustered events with varying stress levels, which form stress peaks marked by vertical dashed lines. More red circles representing very short *DT* for the > 1 kPa data population are shown in Figure 11a, indicating the association between short-term triggering and high-stress perturbation. Such clustering are only sometimes associated with $M > 4$ events in this study area (1989/5 *M*4, 1992/10 *M*4.6, 1993/4 *M*4.5, 1993/11 *M*5.0, 1994/12 *M*5.0), suggesting it is unlikely to be just a consequence of triggering by the $M > 4$ quakes.

[28] To investigate if the numerous short-*DT* events are a result of a big number of background events triggering a few RES events, the temporal distribution of background events and RES events is computed. As shown in Figures 11b and 11c, the stress peaks clusters 1–4 (denoted by vertical dashed lines) are often correlated with peaks in the temporal distribution of RES (Figure 11b), whereas background seismicity does not show a clear association (Figure 11c). In consequence, the observed time-clustered events appear to reflect the clustering of RES events.

[29] But how do we explain the clustered RES events? It could result from static stress triggering by nearby events or aseismic forcing. In order to test the two possibilities, we evaluate if events in a cluster are located close to each other. Figure 12 illustrates the location of RES events in clusters 1–4 by green, red, pink, and yellow stars. Most of the 1987 events in cluster 1 are largely concentrated in a small area of 1×1 km^2, while the other cluster events are more broadly distributed. Cluster 2 occurred close to cluster 1 and shares some common RES as shown by the enlarged view of open box A in Figures 12b and 12c, whereas clusters 3 and 4 are collocated in box B (Figures 12d and 12e). The continuous number of events in boxes A and B indicates that some temporally clustered RES events in Figure 11 can be explained by their spatially adjacent location. A larger number of repeating RESs in close vicinity of each other, therefore, is likely to explain the clustered stress changes in time.

[30] Short-term clustering could also be due to common triggering by a local slow-slip transient spanning the clusters, rather than just short-term triggering between very close-by events. It is difficult to test the presence of such aseismic forcing, but this should probably manifest in a migration of the seismic activity during the swarm episodes. In this case, we expect a certain spatial progression of events in individual clusters. Among the biggest RES swarms (clusters 1–4), we do not find a common/clear migration pattern (Figure 12), leaving the question of clustering by event triggering versus slow-slip event open.

[31] The periodic pulsing of repeating events evident in Figure 11b is widely found along the creeping San Andreas fault [*Nadeau and McEvilly*, 1999; *Nadeau and McEvilly*, 2004]. Deep slip rates derived from RESs in this area reveal cyclic pulses with an interval of 1–2 years, with the first year of the cycle often corresponding to a significant increase in the number of *M*3.5 earthquakes [*Nadeau and McEvilly*, 2004]. During the period of 1993–1998, increases in slip and microseismicity rates and shortened recurrence interval of RES by geodetic and seismic studies were observed at Parkfield [e.g., *Nadeau and McEvilly*, 1999; *Gao et al*., 2000; *Nadeau and McEvilly*, 2004; *Murray and Segall*, 2005; *Chen et al*., 2010a]. These observations suggest that the accelerations in the earthquake occurrence rate and aseismic slip transients in the seismogenic zone are possible drivers of the RES swarms. However, some swarms occurred outside of reported periods of accelerated aseismic slip episodes (e.g., before 1993) and are not correlated with the time of *M*3.5 events, as shown in Figure 11. This suggests that in addition to possible triggering due to $M > 3.5$ events [*Chen et al*., 2010a; Figure 4], swarms of small repeating earthquakes interact with each other so that they tend to occur

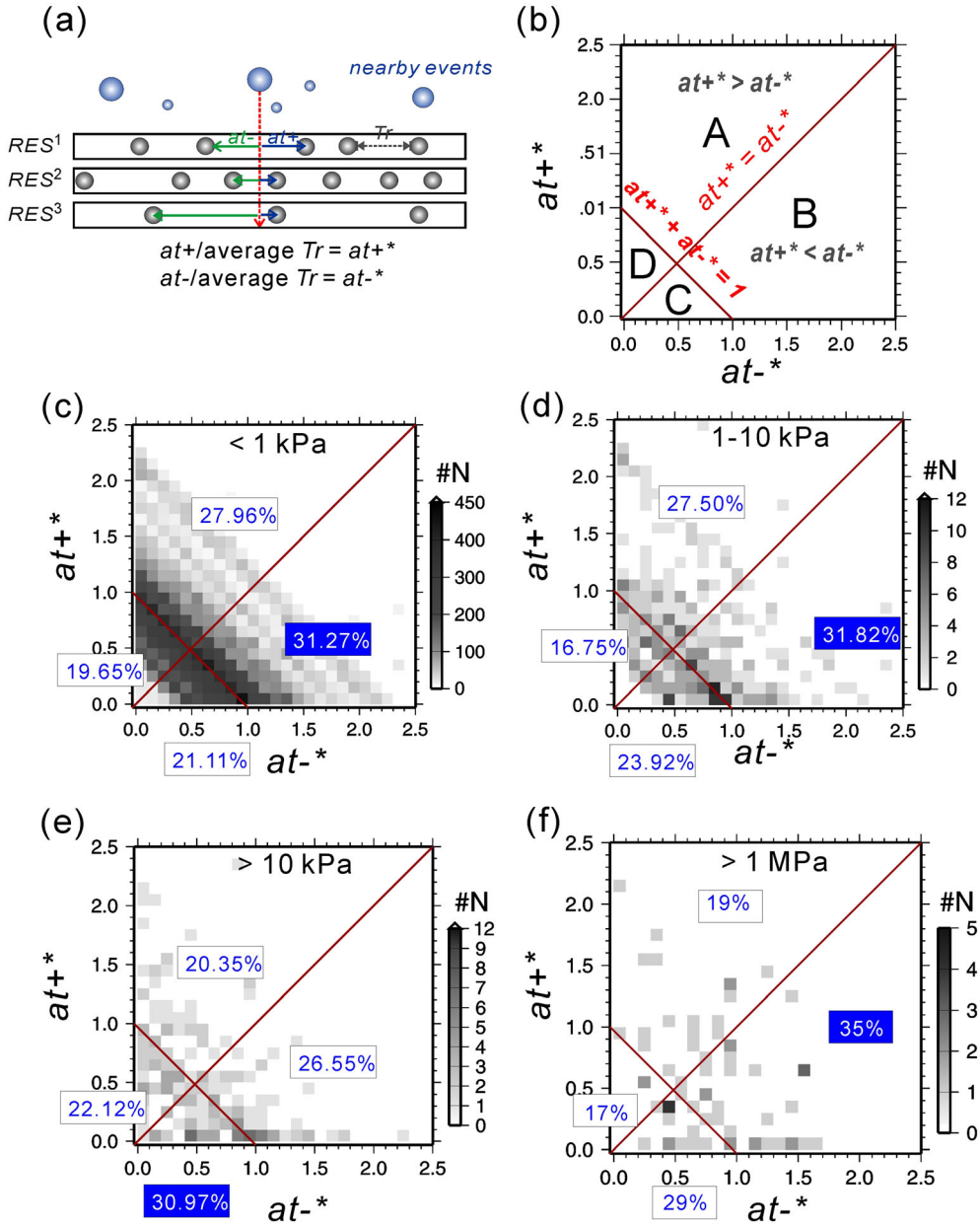

Figure 9. (a) Schematic illustration of the relative time of background event occurrences (including other repeaters and nonrepeating events) with respect to a nearby RES event. Each background event paired with a nearby RES event pair provides both *at*+ and *at*− measurements. (b) Plot of *at*+* versus *at*−* for the RESs. The [*at*+*, *at*−*] data space is divided into four quadrants separated by lines *at*+* + *at*−* = 1 and *at*+* = *at*−*. Red straight lines represent "*at*+* + *at*−* = 1" and "*at*+* = *at*−*," respectively. (c–f) Plot of *at*+* versus *at*−* for the RESs in stress-change ranges of <1 kPa, 1–10 kPa, >10 kPa, and >1 MPa. The number of measures of [*at*+*, *at*−*] in each 0.1 × 0.1 cell are indicated by gray-shaded squares following the scale legend to the right of each plot. Percentage values of numbers in each quadrant are shown in the small boxes.

closely in space and time. Short-term triggering takes place among RESs at short separation distances and plays a role in RES swarm activity.

[32] To further explore if stress interaction between RESs also plays a role in the clustered occurrence of RES events, we next examine the spatial and temporal separations between RES events. Here we consider the time separation and distance between individual repeating events rather than with all nearby earthquakes considered in section 4. Given the varying recurrence intervals among the RESs, we consider the recurrence element "*dt*+" for each RES pair (Figure 13a): the time between one repeating event (the reference RES) and subsequent occurrence of an event in a second RES (the target event). The *dt*+ values are divided by the average pre-Parkfield recurrence interval for the target RES to obtain the normalized values of *dt*+*. For each target event, the normalized

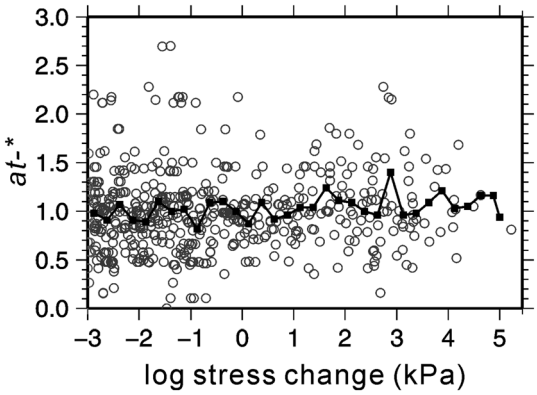

Figure 10. Distribution of *at*−* for preshocks that occurred within 1 day (*at*+ < 1 day) of RES with varying stress change (open circles). Black squares and line indicate the average value of *at*−* in each 0.25 log stress bin.

recurrence element *dt*+* associated with every other RES is calculated. Figure 13b shows the percentage of events within a given stress range (determined by equation (2)) that have a *dt*+* within a given range. We find a dominance of very short *dt*+* at higher stress changes. For example, when considering stress change of 100 kPa, ~14% of the RES pairs have the *dt*+* < 0.1, whereas only 6%, 10%, 8%, and 5% have *dt*+* = 0.1–0.2, 0.2–0.3, 0.3–0.4, and 0.4–0.5, respectively (the remaining ~57% are for the interval *dt*+* > 0.5). Compared to the expected fraction of 10% for 0.1 *dt*+* intervals from randomly chosen earthquakes, the observed *dt*+* <0.1 has a greater percentage for higher stress changes. The difference between the *dt*+* curves starts to be amplified at stress changes >10 kPa and reach a maximum at the peak value considered (10 MPa). The actual number of *dt*+* < 0.1 RES event pairs remains the highest (Figure 13c) compared with other *dt** ranges, suggesting that the higher percentage of *dt*+* <0.1 is not an artifact due to a small sample size. The percentage of short *dt*+* does not change much for events within stress change less than 1 kPa. Pairs with high-stress change are mostly due to shorter separation distance. The distance range for stress change >1 kPa is confined to be about 500 m given the mean magnitude of the RESs and maximum observed inter-RES distance of about 1 km for >1 kPa stress changes. In other words, the triggering effect indicated by our observation

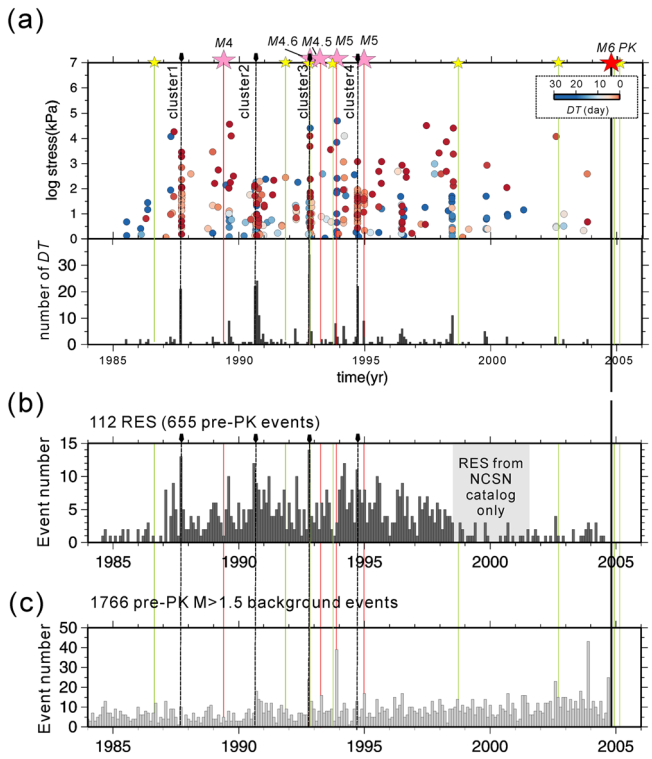

Figure 11. (a) (upper) Temporal distribution of RES events experiencing short-term stress increases from preshocks within a range of *DT*. All 338 preshocks with stress change >1 kPa and *DT* < 30 days (Table 2, Figure 5) are shown. Short-*DT* events are illustrated by red circles (see color scale in inset). *M* > 4 earthquakes are denoted by pink stars and red lines. *M*3.5–4 earthquakes are denoted by yellow stars and green lines. Vertical dashed lines and black arrows indicate stress peaks with numerous >1 kPa stress events (event number greater than 20 in the lower panel showing a histogram of *DT* < 30 day events). (b) Histogram of RES events in 1 month bins. The small number of RES events in 1998–2004 is due to the 1998–2001 data gap in the HRSN RES catalog leading us to only consider pre-gap events from that catalog (Table 1). (c) Time histogram of relocated background seismicity by *Waldhauser et al*. [2004] and *Thurber et al*. [2006]. Only *M* > 1.5 events that occurred prior to the 2004 Parkfield *M*6 earthquake (pre-PK) are shown in Figure 11c.

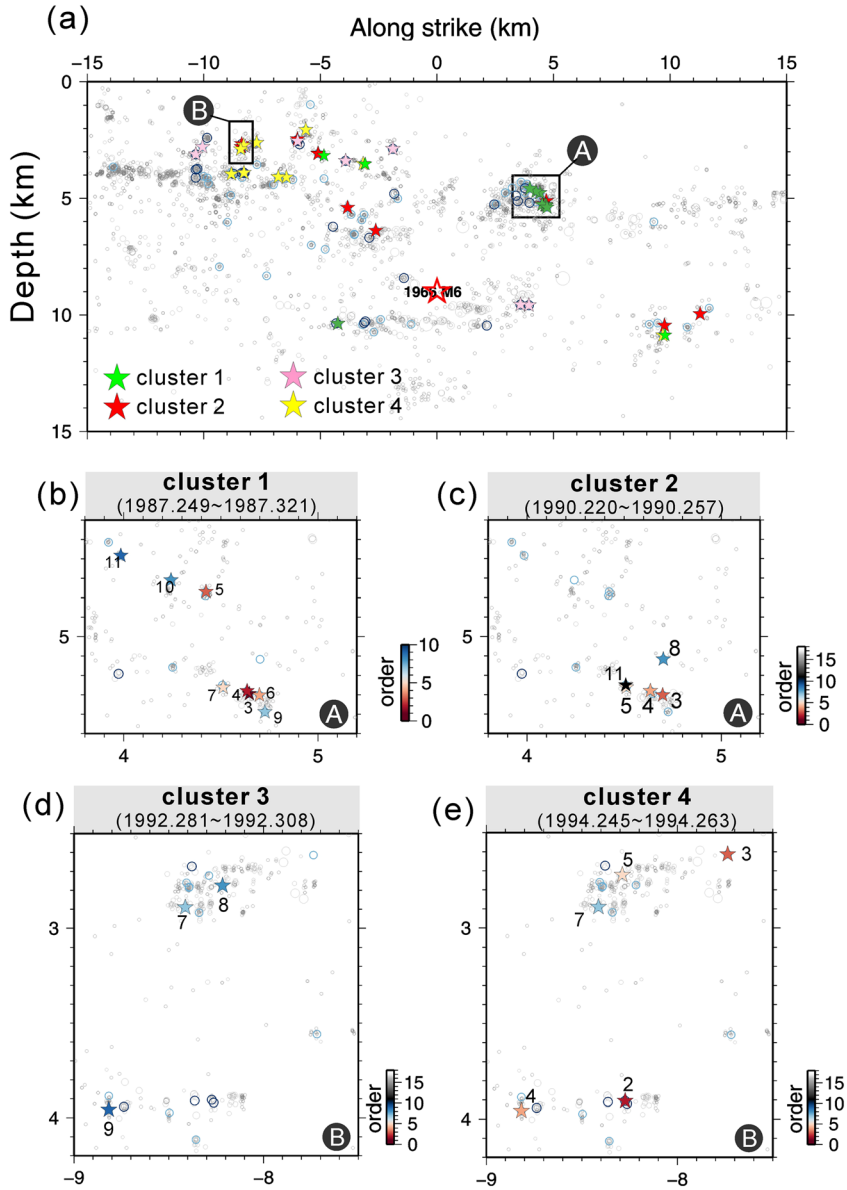

Figure 12. (a) Spatial distribution of repeating event clusters showing stress peaks with numerous >1 kPa stress events (denoted as vertical dashed lines in Figure 11). (b–e) Close-up view for spatially adjacent events in each cluster, color coded by relative order of occurrence in a cluster. Numbers in close-up indicate event ID that defines a temporal order. Relocated background seismicity (1984–2004) is denoted by gray filled circles scaled by event magnitude [*Thurber et al.*, 2006]. For reference, the 1966 *M*6 hypocenter is shown by the open star, and the location of Middle Mountain is labeled as MM at top.

of more than expected dt+* <0.1 event pairs is most evident within a distance of 1 km for the $M \leq 3$ RES in our study area.

7. Discussion

7.1. Short-Term Triggering Induced by Significant Stress Changes

[33] Two different populations of events are examined for evidence of earthquake triggering and interaction: (1) interaction between RES events and background seismicity, where the time difference between an RES event and preceding/following background events is considered as described in sections 4 and 5; and (2) interaction between pairs of RES events, where the time difference between each RES event and preceding/following RES events is evaluated, as described in section 6. Both analyses clearly reveal short-term triggering due to high-stress changes from nearby events.

[34] When considering RES-background seismicity interaction, our calculations reveal a large number of preshocks that trigger RES events within a very short time. Preshocks occurring within 1 day before RES events (time difference >0 in Figure 6) precede 145 of the RES events, suggesting that ~22% of all 655 RES event occurrences are potentially explained by short-term triggering due to nearby events. Of these 145 RES events, 57%, 40%, and 10% were exposed to stress changes from nearby events that are higher than

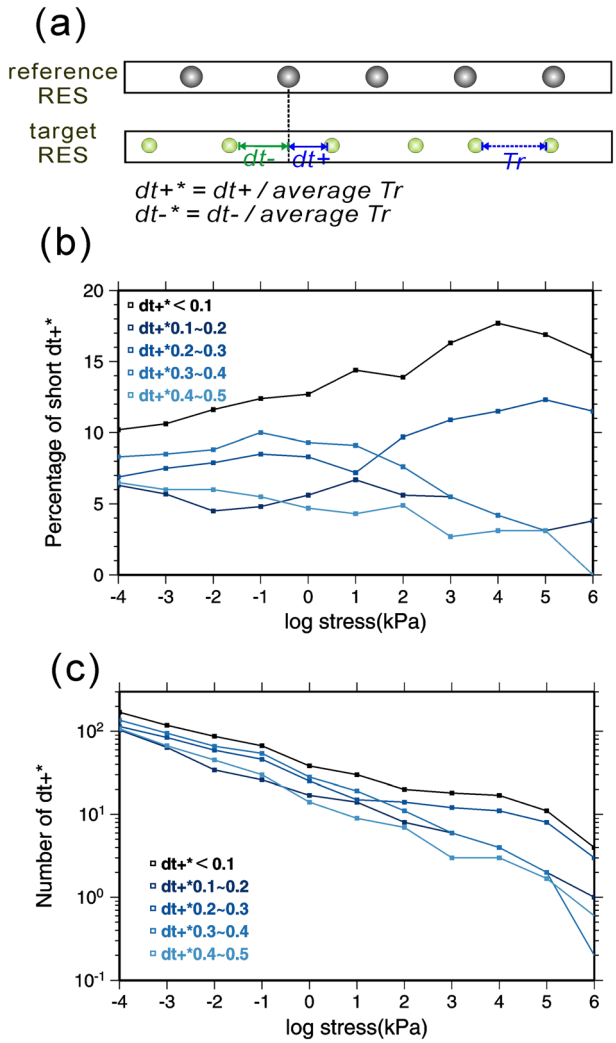

Figure 13. (a) Schematic illustration of the relative time of RES occurrences with respect to a reference RES and the three recurrence elements. Each target RES paired with the reference RES provides a *dt*+ measurement. (b) Percentage of short *dt*+* as a function of stress change. If RES times were randomly distributed, each *dt*+* range would have an equal (10%) chance of occurrence. (c) Number of short *dt*+* as a function of stress change. Lines with different color represent varying selection of normalized time differences between RES pairs (short *dt*+*).

1 kPa, 10 kPa, and 1 MPa, respectively. Peak stress changes by nearby events cause very short-term triggering (Figures 5 and 7). This suggests that short-term triggering as evidenced by earthquake clusters and aftershock sequences plays an important role in the eventual occurrence of an event. We can conclude that the timing of RES events is influenced by preshocks that impose significant stress changes.

[35] When considering RES-RES interaction, the influence zone of RES interaction is confined to less than 1 km, and only 8.4% of repeating events exhibit short-term triggering (*dt*+* < 0.1). If higher stress change is considered (greater than 100 kPa), the fraction of such short-term triggering events are nearly doubled to 14%, suggesting that the RES events exposed to high-stress steps from other RES tend to recur more quickly. However, we argue that only a small portion of RES acceleration activity is attributable to RES-to-RES interaction.

7.2. Relationship between Short-Term Triggering and Earthquake Size

[36] Greater-magnitude events acting as main shocks are often responsible for short-term triggering. Most of the triggered events act as aftershocks, occurring soon after a nearby greater-magnitude preshock. As shown in Figure 6, 60% of stress change >1 kPa preshocks in the 1 day triggering window have greater magnitude than the subsequent RES, and 59% of stress change >1 kPa postshocks have a smaller magnitude than the preceding RES. The bigger-sized nearby earthquakes appear to exhibit a wider influence distance of triggering, as revealed in Figure 8. While Figures 2c and 3b also reveal the bigger-magnitude RES occurring more regularly, we argue that magnitude of RES may play a role in controlling the degree of interaction with nearby events. However, the smaller-sized RES do not always exhibit greater variability in recurrence interval and yet show stronger interaction with neighboring sequences.

[37] A wider range of triggering times for bigger main shocks is evident in Figures 7 and 14, from 1 day to 1 year. We find that a higher occurrence rate of main shock-type preshocks (red line in Figure 14) and aftershock-type postshocks (blue line) appears to last longer than 6 months before falling to background rate values (gray horizontal line). The high occurrence rate drops dramatically in 10 days and slowly decreases to background rate level of 1.5 events per day. The triggering/clustering out to longer times of 6 months may partly reflect the coherent acceleration of event occurrences associated with the pulsed occurrence of RES events [*Nadeau and McEvilly*, 2004] and longer periods of accelerated fault slip and seismicity associated with *M*4–5 events at Parkfield [e.g., *Nadeau and McEvilly*, 1999]. We argue that the size of nearby events have impact on the triggering distance and time but not the variability of recurrence intervals.

7.3. Effect of Stress Changes on Tr and Caveats of Static Calculations

[38] Three mechanisms are known to produce very short apparent or actual recurrence intervals. These mechanisms include (1) apparent short intervals produced by cross-triggering of events between distinct yet closely spaced repeating asperities when events on the different asperities are taken as occurring on a single asperity, either intentionally or due to insufficient spatial resolution [*Nadeau et al.*, 1995; *Waldhauser and Ellsworth*, 2002; *Nadeau and McEvilly*, 2004; *Bourouis and Bernard*, 2007; *Lengline and Marsan*, 2009], (2) short intervals resulting from high aseismic slip loading rates (e.g., afterslip from a nearby large event) [*Vidale et al.*, 1994; *Schaff et al.*, 1998], and (3) relatively rare burst-type recurrence behavior where short intervals occur by a local increase in stress due to the occurrence of large nearby earthquakes and do not reflect the background creep rate of the fault [*Kimura et al.*, 2006; *Templeton et al.*, 2008].

[39] There are only a few very short recurrence intervals in our data set. Our RES identification resolves repeated events on individual asperities so that the cross-triggering mechanism is likely not responsible. There were also no events larger than ~*M*5 during the observation period, so that the

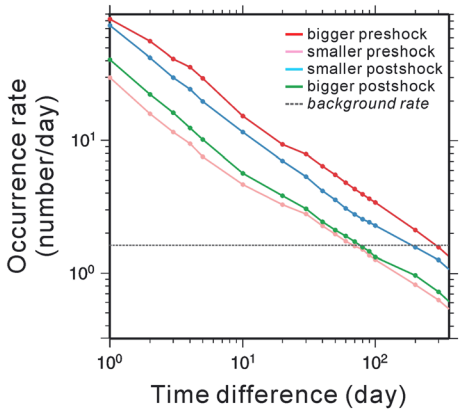

Figure 14. Occurrence rate of >1 kPa preshock and postshock in varying time window from the RES events. Preshocks with bigger and smaller magnitude than the following RES events are shown by red and pink lines, respectively. Postshock with smaller and bigger magnitude than the preceding RES events are shown by blue and green blue lines, respectively. The background rate (1.5/day) is calculated from the events that occur from 1 to 10 years from the RES events.

other mechanisms mentioned may have been responsible locally in the few cases that are observed.

[40] Here we find that the well-documented short-term triggering only leads to a modest reduction in recurrence intervals of the triggered RES events, as illustrated in Figures 9 and 10. Many triggered RES events were already late in their earthquake cycle as indicated by the distribution of $at-*$ values centered around 1 shown in Figure 10. Some of the short-term triggered events occurred after recurrence intervals as short as 40% of the mean value of the corresponding sequence, while others followed greater-than-average intervals. RES events triggered by greater stress steps do not include a larger fraction of repeaters that recur prematurely (Figure 10).

[41] We see only modest effects of static stress changes on RES events in their eventual recurrence intervals. About 22% of the RES show ~20% shortened recurrence interval during the period of the reported slip transient of 1993 to 1998 [*Chen et al.*, 2010a], suggesting that larger scale deformation transients play a more important role in determining earthquake recurrence intervals than interaction between events.

[42] When we consider the total stress change from neighboring events experienced by an RES between two recurrences, we only see a significant reduction of recurrence intervals for very large stress values (Figure 3). The poor correlation between normalized *Tr* and stress perturbation can be explained by (1) the role of time-dependent creep rate variations, (2) over-estimate of some *Tr* due to missing repeating events in the catalog [*Chen et al.*, 2010a], possibly indicated by some very large normalized *Tr* shown in Figures 3c and 3d, (3) uncertainties in earthquake location and stress from nearby small events not included in our catalog, and (4) errors in the stress estimates due to simplifying model assumptions. In this study, we determine the static stress change by assuming seismicity in Parkfield along a single fault plane. Such stress changes are simply a function of distance and magnitude of triggering events. This should be further explored in future studies by considering the full 3D relative event locations and stress fields and the role of multiple subparallel fault planes [*Rubin et al.*, 1999; *Thurber et al.*, 2004; *Waldhauser et al.*, 2004]. Also note that smaller than *M*1.6 earthquakes that are not completely reported in the double-difference relocation catalog (completeness of magnitude reported in *Woessner et al.* [2006]) might also have an important stress effect, which cannot be resolved in the current study.

7.4. Static, Afterslip, and Dynamic Triggering

[43] The stress change from 1 day triggering events versus distance pattern is shown in Figure 15. The higher stress values of >1 kPa correspond to short separation distances of less than ~1 km (denoted by dashed red line and red arrow in Figure 15), while the apparent short-term triggering at >30 kPa identified in Figure 6 corresponds to ~0.5 km separation distance (dashed blue line and blue arrow). There is an upper bound of separation distance at 0.5 km for events under extreme stress changes (greater than 1000 kPa), as indicated by the green arrow in Figure 15. These results are compared with the decaying functions $1/r^3$ and $1/r$ as illustrated by thick and thin lines in Figure 15, respectively, corresponding to static (equation (2)) and dynamic [*Cotton and Coutant*, 1997] stress-change values computed for the mean event magnitude (*M*1.32) of the RES events. The stress changes from 1 day triggering events appear to fit the static stress change model but with a slightly faster rate of decay. This suggests that static stress increases from the trigger-event rupture plays an important role in short-term triggering but may not be the only significant factor. Note that the short-term stress triggering also reveals the effect of triggering event magnitude; the influence zone changes from 1 km to 4 km for triggering events of $M < 2$ to $M > 4$

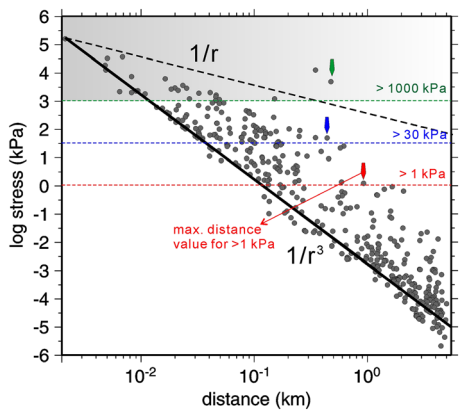

Figure 15. Distance as a function of stress change for 1 day triggering events (preshock + postshock). The scatter in values is due to the range in moments of the source events. Black bold and thin lines indicate the static (decaying as $1/r^3$) and dynamic ($1/r$) stress changes, respectively, which are induced by RES with the mean seismic moment (equivalent to an *M*1.32) of the 655 RES events [*Cotton and Coutant*, 1997]. Gray box indicates the stress change >1000 kPa. Dashed red, blue, and green lines indicate the stress change of 1 kPa, 30 kPa, and 1000 kPa, respectively. The maximum separation distances for a given stress change range are denoted by arrows.

as illustrated in Figure 8. This implies that both static stress increases and aseismic afterslip play the primary role in the observed short-term triggering. A model where increases in earthquake magnitude result in a wider triggering distance is consistent with our observations. As dynamic stresses decay more slowly with distance [*Helmstetter et al*., 2005], they may play an additional role in interaction between small events, as suggested by studies of near-field triggering [*Felzer and Brodsky*, 2006; *Parsons and Velasco*, 2009; *van der Elst and Brodsky*, 2010]. However, by simply checking the distance versus time relation for all background events that occurred within 1 day of the RES, we find no events that occurred immediately during the passage of seismic waves indicative of direct dynamic triggering (Figure S2). It is possible that very small aftershocks not included in the catalog or dynamically triggered slow slip could produce delayed dynamic triggering. Here we make no further attempt to discriminate static from dynamic stress triggering; instead, we point out that first-order consideration of distance and magnitude dependent static stress changes help explain the triggering of small RES and nearby background earthquakes, while delayed dynamic stress triggering cannot be ruled out.

8. Conclusion

[44] We examined the timing of precisely relocated RESs and nearby earthquakes at a fine scale in an attempt to identify systematic interaction and to infer the possible role of static stress changes behind it. We find that quasi-periodic RESs tend to be isolated in space, away from the rupture zone of $M > 4$ events. The regularity of a RES can be perturbed if there are a large number of nearby events. The variability of recurrence interval, however, is not clearly correlated with total stress change from nearby events. A modest but significant shortening of recurrence intervals is taking place when estimated average stressing rates due to neighboring earthquakes during a recurrence interval exceed 1 MPa per year.

[45] When static stress changes induced by nearby events are computed for varying time spans before and after an RES event, we find that a large number of events producing stress changes >1 kPa occur during $|DT| \leq 5$ days, indicating short-term triggering. Immediate triggering within a few seconds to minutes can also happen when the separation distance is less than a few kilometers. When earthquakes are separated by longer distances, their communication (triggering) becomes less efficient. An apparent preponderance of triggering of RES events over time spans as small as 1 day is evident when the stress change imposed on the RES site is higher than ~30 kPa. As the time difference gets shorter, the relative contribution of very high-stress change events increases. The impact on the time to be triggered is related to the relative size of triggered and triggering events. Preshocks that are larger than the RES events produce much of the short-term triggering; that is, the triggered RES events are aftershocks. In addition, we find that short-term triggering involves RES events that on average are relatively late in their respective earthquake cycle. However, the most recent recurrence intervals of short-term triggered events span a wide range and do not appear strongly influenced by the magnitude of the trigger stress. Groups of nearby small repeating earthquakes tend to occur in temporal clusters, suggesting correlated behavior due to short-term interaction or triggering by slow-slip transients.

[46] Consequently, we find that ~22% of all 655 RES event occurrences are potentially explained by short-term triggering (i.e., >1 kPa preshocks occurring within 1 day before the RES events), whereas ~6% are likely explained by active swarm associated with aseismic transient (indicated by arrows in Figure 11). In our dataset, none of them act as clear candidates for immediate dynamic triggering. There are other mechanisms that can be also added to the direct effect of static stress changes on the timing of earthquake recurrences like very small aftershocks not included in the earthquake catalogs.

[47] Our results show how the interaction between repeating earthquake sequences and nearby events controls the recurrence timing. By considering the distribution of event recurrence intervals, separation distances, relative sizes, loading rate, and event timing of real Parkfield events, one should be able to explicitly model the mechanics of such interactions and test prospective forecasts by comparing the success of predictions of future event recurrence times in the future.

[48] **Acknowledgments.** We are grateful to Bruce Shaw, Terry Tullis, Bill Ellsworth, Justin Rubinstein, Zhigang Peng, Ross Stein, Shinji Toda, and Ting Chen for helpful discussions. This work was supported by a Southern California Earthquake Center grant (contribution number 1687), the National Science Foundation through grants EAR-0738342 and EAR-0910322, Taiwan NSC grant NSC 100-2119-M-003-0062. The Parkfield High-Resolution Seismic Network (HRSN) is operated by University of California, Berkeley Seismological Laboratory with financial support from the US Geological Survey (USGS) grant G10AC00093. Seismic data are archived at the Northern California Earthquake Data Center. This is Berkeley Seismological Laboratory contribution 12–17.

References

Anooshehpoor, A., and J. N. Brune (2001), Quasi-static slip-rate shielding by locked and creeping zones as an explanation for small repeating earthquakes at Parkfield, *Bull. Seismol. Soc. Am.*, *91*(2), 401–403.

Beeler, N. M., T. E. Tullis, and J. D. Weeks (1994), The roles of time and displacement in the evolution effect in rock friction, *Geophys. Res. Lett.*, *21*, 1987–1990.

Beeler, N. M., D. L. Lockner, and S. H. Hickman (2001), A simple stick-slip and creep-slip model for repeating earthquakes and its implication for microearthquakes at Parkfield, *Bull. Seismol. Soc. Am.*, *91*(6), 1797–1804.

Berryman, K. R, U. A. Cochran, K. J. Clark, G. P. Biasi, R. M. Langridge, P. Villamor (2012), Major earthquakes occur regularly on an isolated plate boundary fault, *Science*, *336*(6089), 1690–1693.

Bourouis, S., and P. Bernard (2007), Evidence for coupled seismic and aseismic fault slip during water injection in the geothermal site of Soultz (France), and implications for seismogenic transients, *Geophy. J. Int.*, *169*, 723–732.

Bürgmann, R., D. Schmidt, R. M. Nadeau, M. d'Alessio, E. Fielding, D. Manaker, T. V. McEvilly, and M. H. Murray (2000), Earthquake potential along the Northern Hayward Fault, California, *Science*, *289*, 1178–1182.

Chen, K. H., R. Bürgmann, and R. M. Nadeau (2010a), Triggering effect of *M* 4–5 earthquakes on the earthquake cycle of repeating events at Parkfield, California, *Bull. Seismol. Soc. Am.*, *100*, 2, doi:10.1785/0120080369.

Chen, K. H., R. Bürgmann, R. M. Nadeau, T. Chen, N. Lapusta (2010b), Postseismic variations in seismic moment and recurrence interval of repeating earthquakes, *Earth Planet. Sci. Lett.*, *299*, 118–125, doi:10.1016/j.epsl.2010.08.027.

Chen, K. H., R. M. Nadeau, and R. J. Rau (2007), Towards a universal rule on the recurrence interval scaling of repeating earthquakes?, *Geophys. Res. Lett.*, *34*, L16308, doi:10.1029/2007GL030554.

Chen, K. H., R. M. Nadeau, and R. J. Rau (2008), Characteristic repeating earthquakes in an arc-continent collision boundary zone—the Chihshang fault of eastern Taiwan, *Earth Planet. Sci. Lett.*, *276*, doi:10.1016/j.epsl.2008.09.021.

Cotton F., and Coutant O. (1997), Dynamic stress variations due to shear faults in a plane-layered medium, *Geophys. J. Int.*, *128*, 676–688.

Dieterich, J. H. (1972), Time-dependent friction in rocks, *J. Geophys. Res.*, *77*, 3690–3697.

Ellsworth, W. L. (1995), Characteristic earthquakes and long-term earthquake forecasts: Implications of central California seismicity, in *Urban Disaster Mitigation: The Role of Engineering and Technology*, edited by F. Y. Cheng and M. S. Sheu, Elsevier, pp. 1–14.

Ellsworth, W. L., M. V. Matthews, R. M. Nadeau, S. P. Nishenko, P. A. Reasenberg, and R. W. Simpson (1999), A physically-based earthquake recurrence model for estimation of long-term earthquake probabilities, *U.S. Geol. Surv. Open-File Rep.* 99–522.

Felzer, K. R., and E. E. Brodsky (2006), Decay of aftershock density with distance indicates triggering by dynamic stress, *Nature*, *441*, 735–738.

Freed, A. M. (2005), Earthquake triggering by static, dynamic, and postseismic stress transfer, *Annu. Rev. Earth Planet. Sci.*, *33*, 335–367.

Gao, S., P. G. Silver, and A. T. Linde (2000), Analysis of deformation data at Parkfield, California: Detection of a long-term strain transient, *J. Geophys. Res.*, *105*(B2), 2955–2967.

Hill, D., et al. (1993), Seismicity remotely triggered by the magnitude 7.3 Landers, California, earthquake, *Science*, *260*, 1617–1623.

Harris, R. A. (1998), Introduction to special section: Stress triggers, stress shadows, and implications for seismic hazard, *J. Geophys. Res.*, *103*, 24,347–24,358.

Helmstetter, A., Y. Y. Kagan, and D. D. Jackson (2005), Importance of small earthquakes for stress transfers and earthquake triggering, *J. Geophys. Res.*, *110*, B05S08, doi:10.1029/2004JB003286.

Igarashi, T., T. Matsuzawa, and A. Hasegawa (2003), Repeating earthquakes and interplate aseismic slip in the northeastern Japan subduction zone, *J. Geophys. Res.*, *108*, doi:10.1029/2002JB001920.

Johnson, L. R., and R. M. Nadeau (2002), Asperity model of an earthquake: Static problem, *Bull. Seismol. Soc. Am.*, *92*(2), 672–686.

Kimura, H., K. Kasahara, T. Igarashi, and N. Hirata (2006), Repeating earthquake activities associated with the Philippine Sea plate subduction in the Kanto district, central Japan: A new plate configuration revealed by interpolate aseismic slips, *Tectonophysics*, *417*, 101–118.

Lay, T., and H. Kanamori (1980), Earthquake doublets in the Solomon Islands, *Phys. Earth Planet. Inter.*, *21*, 283–304.

Lengliné, O., and D. Marsan (2009), Inferring the coseismic and postseismic stress changes caused by the 2004 $M_w = 6$ Parkfield earthquake from variations of recurrence times of microearthquakes, *J. Geophys. Res.*, *114*, B10303, doi:10.1029/2008JB006118.

Marone, C. (1998), Laboratory-derived friction laws and their application to seismic faulting, *Annu. Rev. Earth Planet. Sci.*, *26*, 643–696.

Marone, C., J. E. Vidale, and W. L. Ellsworth (1995), Fault healing inferred from time dependent variations in source properties of repeating earthquakes, *Geophys. Res. Lett.*, *22*, 3095–3098.

Matsuzawa, T., T. Igarashi, and A. Hasegawa (2002), Characteristic small-earthquake sequence off Sanriku, northeastern Honshu, Japan, *Geophys. Res. Lett.*, *29*(11), doi:10.1029/2001GL014632.

Murray, J., and P. Segall (2005), Spatiotemporal evolution of a transient slip event on the San Andreas fault near Parkfield, *J. Geophys. Res.*, *110*, B09407, doi:10.1029/2005JB003651.

Nadeau, R. M., and L. R. Johnson (1998), Seismological Studies at Parkfield VI: Moment release rates and estimates of source parameters for small repeating earthquakes, *Bull. Seismol. Soc. Am.*, *88*, 790–814.

Nadeau, R. M., and T. V. McEvilly (1997), Seismological studies at Parkfield V: Characteristic microearthquake sequences as fault-zone drilling targets, *Bull. Seismol. Soc. Am.*, *87*, 1463–1472.

Nadeau, R. M., and T. V. McEvilly (1999), Fault slip rates at depth from recurrence intervals of repeating microearthquakes, *Science*, *285*(5428), 718–721.

Nadeau, R. M., and T. V. McEvilly (2004), Periodic pulsing of characteristic microearthquakes on the San Andreas fault, *Science*, *303*, 220–222.

Nadeau, R. M., W. Foxall, and T. V. McEvilly (1995), Clustering and periodic recurrence of microearthquakes on the San Andreas fault at Parkfield, *California, Science*, *267*, 503–507.

Nadeau R. M., A. Michelini, R. A. Uhrhammer, D. Dolenc, T. V. McEvilly (2004), Detailed kinematics, structure and recurrence of micro-seismicity in the SAFOD target region, *Geophys. Res. Lett.*, *31*, L12S08, doi:10.1029/2003GL019409.

Okada, Y. (1992), Internal deformation due to shear and tensile faults in a half space, *Bull. Seismol. Soc. Am.*, *82*, 1018–1040.

Parsons, T., and A. A. Velasco (2009), On near-source earthquake triggering, *J. Geophys. Res.*, *114*, B10307, doi:10.1029/2008JB006277.

Peng, Z., and Y. Ben-Zion (2005), Spatio-temporal variations of crustal anisotropy from similar events in aftershocks of the 1999 M7.4 Izmit and M7.1 Düzce, Turkey, earthquake sequences, *Geophys. J. Int.*, *160*(3), 1027–1043, doi:10.1111/j.1365-246X.2005.02569.x.

Peng, Z., J. E. Vidale, C. Marone and A. Rubin (2005), Systematic variations in recurrence interval and moment of repeating aftershocks, *Geophys. Res. Lett.*, *32*, L15301, doi:10.1029/2005GL022626.

Richards-Dinger, K., R. S. Stein, and S. Toda (2010), Decay of aftershock density with distance does not indicate triggering by dynamic stress, *Nature*, *467*, doi:10.1038/nature09402.

Rubin, A. M., D. Gillard, and J.-L. Got (1999), Streaks of microearthquakes along creeping faults, *Nature*, *400*, 635–641.

Sammis, C. G., R. M. Nadeau, and L. R. Johnson (1999), How strong is an asperity? *J. Geophys. Res.*, *104*, 10,609–10,619.

Schaff, D. P., G. C. Beroza, and B. E. Shaw (1998), Postseismic response of repeating aftershocks, *Geophys. Res. Lett.*, *25*(24), 4549–4552, doi:10.1029/1998GL900192.

Sykes, L. R., and W. Menke (2006), Repeat times of large earthquakes: Implications for earthquake mechanics and long-term prediction, *Bull. Seismol. Soc. Am.*, *96*, 1569–1596, doi:10.1785/0120050083.

Sleep, N.H., and M. L. Blanpied (1994), Ductile creep and compaction: A mechanism for transiently increasing fluid pressure in mostly sealed fault zones, *Pure Appl. Geophys.*, *143*, 9–40.

Stein, R. S. (2003), Earthquake conversations, *Sci. Am.*, *288*, 72–79.

Taira, T., P. G. Silver, F. Niu, R. M. Nadeau (2009), Remote triggering of fault-strength changes on the San Andreas fault at Parkfield, *Nature*, *461*, 636–639, doi:10.1038/nature08395.

Templeton, D.C., R. M. Nadeau, and R. Bürgmann (2008), Behavior of repeating earthquake sequences in Central California and the implications for subsurface fault creep, *Bull. Seismol. Soc. Am.*, *98*(1), 52–65.

Templeton, D.C., R. M. Nadeau, and R. Bürgmann (2009), Distribution of postseismic slip on the Calaveras fault, California, following the 1984 M6.2 Morgan Hill earthquake, *Earth Planet. Sci. Lett.*, *277*, 1–8, doi:10.1016/j.epsl.2008.09.024.

Thurber, C., S. Roecker, H. Zhang, S. Baher, and W. Ellsworth (2004), Fine-scale structure of the San Andreas fault zone and location of the SAFOD target earthquakes, *Geophys. Res. Lett.*, *31*, L12S02, doi:10.1029/2003GL019398.

Thurber, C., H. Zhang, F. Waldhauser, J. Hardebeck, A. Michael, and D. Eberhart-Phillips (2006). Three-dimensional compressional wavespeed model, earthquake relocations, and focal mechanisms for the Parkfield, California, region, *Bull. Seismol. Soc. Am.*, *96*(4B), S38–S49.

Toda, S., R. S. Stein, G. C. Beroza, D. Marsan (2012), Aftershocks halted by static stress shadows, *Nature Geoscience*, doi:10.1038/ngeo1465.

Uchida, N., T. Matsuzawa, A. Hasegawa, and T. Igarashi (2003), Interplate quasi-static slip off Sanriku, NE Japan, estimated from repeating earthquakes, *Geophys. Res. Lett.*, *30*(15), 1801, doi:10.1029/2003GL017452.

van der Elst, N. J., and E. E. Brodsky (2010), Connecting near-field and far-field earthquake triggering to dynamic strain, *J. Geophys. Res.*, *115*, B07311, doi:10.1029/2009JB006681.

Velasco, A. A., S. Hernandez, T. Parsons, and K. Pankow (2008), Global ubiquity of dynamic earthquake triggering, *Nature Geoscience*, *1*, 375–379, doi:10.1038/ngeo204.

Vidale, J. E., W. L. Ellsworth, A. Cole, and C. Marone (1994), Variations in rupture process with recurrence interval in a repeated small earthquake, *Nature*, *368*, 624–626.

Waldhauser, F., and W. L. Ellsworth (2002), Fault structure and mechanics of the Hayward Fault, California, from double-difference earthquake locations, *J. Geophys. Res.*, *107*(B3), 2054, doi:10.1029/2000JB000084.

Waldhauser, F., W. Ellsworth, D. P. Schaff, and A. Cole (2004), Streaks, multiplets, and holes: High-resolution spatio-temporal behavior of Parkfield seismicity, *Geophys. Res. Lett.*, *31*, L18608, doi:10.1029/2004GL020649.

Woessner, J., D. Schorlemmer, S. Wiemer, and P. M. Mai (2006), Spatial correlation of aftershock locations and on-fault main shock properties, *J. Geophys. Res.*, *11*, B08301, doi:10.1029/2005JB003961.